Long-Range Electron Transfer in Engineered Azurins Exhibits Marcus Inverted Region Behavior

ARTICLE *in* JOURNAL OF PHYSICAL CHEMISTRY LETTERS · DECEMBER 2014

Impact Factor: 7.46 · DOI: 10.1021/jz5022685

6 AUTHORS, INCLUDING:

Parisa Hosseinzadeh
University of Illinois, Urbana-Champaign
7 PUBLICATIONS **52** CITATIONS
SEE PROFILE

Yi Lu
Nanjing University
399 PUBLICATIONS **14,758** CITATIONS
SEE PROFILE

THE JOURNAL OF PHYSICAL CHEMISTRY Letters

Letter

pubs.acs.org/JPCL

Long-Range Electron Transfer in Engineered Azurins Exhibits Marcus Inverted Region Behavior

Ole Farver,[†] Parisa Hosseinzadeh,[‡] Nicholas M. Marshall,[⊥] Scot Wherland,[∥] Yi Lu,*[,‡,⊥] and Israel Pecht[§]

[†]Department of Analytical and Bioinorganic Chemistry, University of Copenhagen, Universitetsparken 5, Copenhagen 2100, Denmark

[‡]Department of Biochemistry and [⊥]Department of Chemistry, University of Illinois at Urbana−Champaign, 600 South Mathews Avenue, Urbana, Illinois 61801, United States

[∥]Department of Chemistry, Washington State University, PO Box 644630, Pullman, Washington 99164, United States

[§]Department of Immunology, Weizmann Institute of Science, Wolfson Building, Rehovot 76100, Israel

Supporting Information

ABSTRACT: The Marcus theory of electron transfer (ET) predicts that while the ET rate constants increase with rising driving force until it equals a reaction's reorganization energy, at higher driving force the ET rate decreases, having reached the Marcus inverted region. While experimental evidence of the inverted region has been reported for organic and inorganic ET reactions as well as for proteins conjugated with ancillary redox moieties, evidence of the inverted region in a "protein-only" system has remained elusive. We herein provide such evidence in a series of nonderivatized proteins. These results may facilitate the design of ET centers for future applications such as advanced energy conversions.

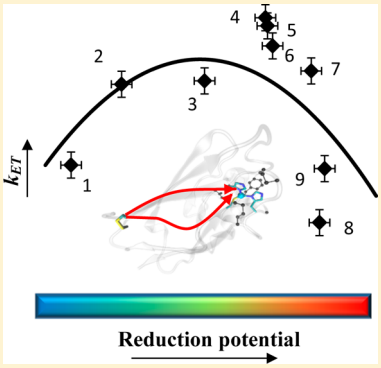

Understanding the parameters that control electron transfer (ET) rates in biomolecules is of fundamental importance in chemistry and biology.[1−9] Nature has optimized the structures, separation distances, and driving forces of donors and acceptors to ensure facile and efficient ET in biological processes,[10−12] and a large number of studies have focused on understanding the factors controling these rates.[13−19] The semiclassical Marcus theory states that three parameters determine the rate of ET between a donor and an acceptor held at a fixed distance and orientation: the electronic coupling between the reactants, their reorganization energy, and the driving force of the reaction.[20,21] A counterintuitive result of the theory is its prediction of a Gaussian dependence of the ET rates on driving force, namely, that while the ET rate constants increase with rising driving force until it equals the reorganization energy, at higher driving force the rate constants decrease, reaching the "Marcus inverted region". Three decades elapsed until the inverted region was experimentally observed by Miller, Calcaterra, and Closs in 1984[22] using a series of organic donor−acceptor molecules. This was further established in an inorganic model system of an iridium(I) dimer by Gray et al.[23] The search for an inverted region within proteins was pioneered by Durham, Millett, and coworkers[24] using ruthenium-labeled cytochrome b_5, and by Gray and coworkers employing singlet and triplet excited states of a zinc-substituted cytochrome *c*.[25]

Since these reports were published, experimental evidence for the "inverted region" behavior in a nonderivatized protein has remained elusive. Such experimental evidence is of considerable interest because the inverted region has been proposed to be responsible for a number of crucial biological ET processes in proteins, such as the charge separation in photosynthetic reaction centers, and was experimentally observed through replacement of the native quinones at the QA site of the reaction center protein from *Rhodobacter sphaeroides*.[26,27]

An optimal system for pursuing such a challenge is the bacterial ET protein azurin (Az) that contains a blue type 1 (T1) copper center coordinated by three strong ligands, His46, Cys112, and His117, in a trigonal planar geometry around the Cu center. A large number of biochemical and biophysical studies, including spectroscopic, X-ray crystallographic, and computational studies of both wild type (WT) Az and its mutants, have resulted in thorough understanding of 3-D and electronic structures responsible for its ET function.[28−35] Of particular interest are those Az mutants whose reduction potentials have been tuned to allow a wide range of driving forces for ET reactions.[36−41] Recently we produced Az mutants where its primary coordination sphere is kept intact while the

Received: October 27, 2014
Accepted: December 8, 2014
Published: December 8, 2014

weaker axial ligand, Met121, was replaced by Gln or Leu to tune the hydrophobicity around the copper.[42] In addition, Asn47 was replaced by Ser and Phe114 by Asn or Pro to modify the hydrogen bonding networks around the Cys112 and His117 copper ligands, respectively.[42] These changes modulated the reduction potential of the Cu site over a wide range (>500 mV) without significantly disrupting the coordination site. To investigate how the changes in the Cu(II) site's reduction potential influence its reorganization energy, we have previously measured the intramolecular ET rates in Az from a disulfide radical anion, produced by pulse radiolysis, to the Cu(II) center in several of these mutants.[43] Indeed we found that the ET proceeds with lower reorganization energy than in WT Az.

To enable a quantitative examination of the relationship between the ET, driving force, and the rate constant in a protein-only system without any ancillary foreign donor or acceptor, we have now expanded this series and prepared several other mutants (F114N, N47S/F114S/M121L, and M44F/N47S/F114N/G116F) with higher potentials than that of WT Az (Figure 1 and Table 1).

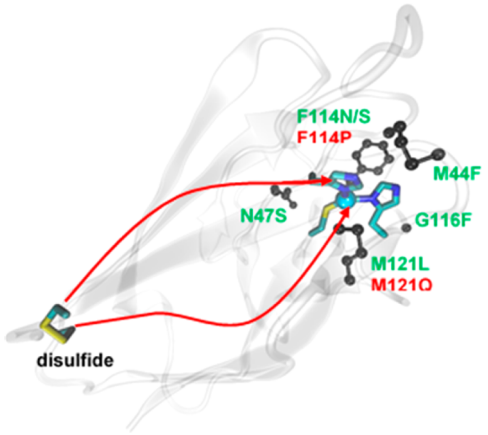

Figure 1. Schematic presentation of Az and the designed mutants. Calculated paths (see below) of electron transfer from the disulfide to Cu are illustrated by the red arrows. The mutated residues are shown in black sticks and balls. The green mutations cause an increase in reduction potential, while the red ones decrease it.

Kinetic measurements of the intramolecular ET in these nine different Az mutants, including three previously unreported ones with reduction potentials from 0.39 to 0.61 V versus NHE, have been investigated. Pulse radiolytically produced CO_2^- radicals reduce both the disulfide bridge (Cys3−Cys26) and the Cu(II) site in Az with similar, essentially diffusion-controlled rate constants ($k_1 \approx 10^9$ M^{-1} s^{-1}), (Figure 2).

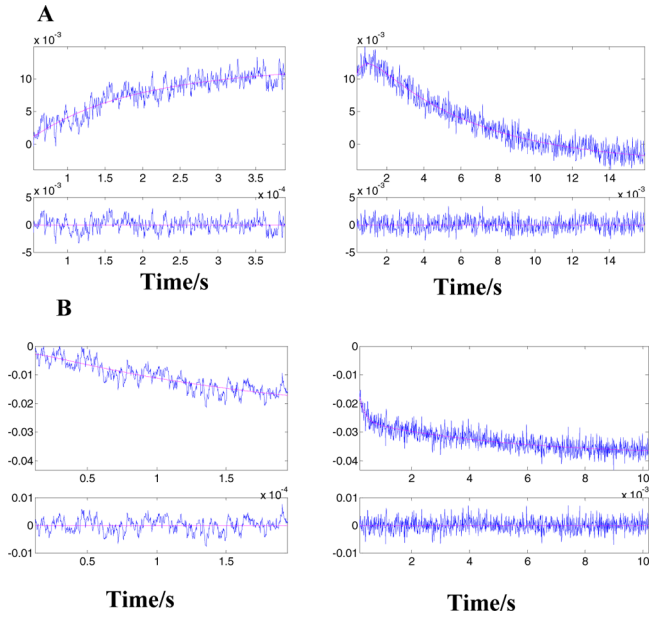

Figure 2. (A) Time-resolved absorption changes at 410 nm of the F114N azurin mutant, monitoring the formation and decay of the RSS·R⁻ radical ions. (B) Time-resolved absorption changes (625 nm) of the F114N Az mutant monitoring reduction of Cu(II). The protein concentration was 93 μM in a N_2O-saturated solution; temperature 25 °C. All other technical details are described in the experimental methods in the Supporting Information.

Because an excess of protein is employed over the reducing CO_2^- radicals, only a fraction of either disulfide or Cu(II) is reduced, allowing for the disulfide radical produced (RSS·R⁻) to transfer an electron to the Cu(II) center in a second slower and concentration-independent, intramolecular ET process (Figure 2)

$$\text{Az[Cu(II)RSS}^{\cdot}\text{R}^-] \xrightarrow{k_{ET}} \text{Az[Cu(I)RSSR]}$$

The rate constants, k_{ET}, at 25 °C were determined by monitoring both the oxidation of the radical (410 nm, Figure 2A) and reduction of Cu(II) (600−635 nm, depending on the mutant's absorption maximum, Figure 2B). The k_{ET} values and calculated activation parameters are presented in Table 1 together with earlier results.

Calculations of ET pathways between the RSS·R⁻ radical ion and Cu(II) in these mutants showed that the same two

Table 1. Rate Constants, Activation Parameters of the Intramolecular ET Reactions, and the Potentials of the Copper Site

azurin mutant	k_{ET} (s^{-1}) at 298 K	$E°$ (mV)	$\Delta H^‡$ (kJ/mol)	$\Delta S^‡$ (J/K·mol)
1. F114P/M121Q[a]	81 ± 11	122 ± 6	36.6 ± 7.5	−86 ± 14
2. F114P[a]	191 ± 26	220 ± 18	~29	−106
3. F114N[b]	198 ± 14	381 ± 8	29.9 ± 0.2	−101 ± 1
4. N47S/F114N[a]	387 ± 59	499 ± 3	33.7 ± 2.5	−82 ± 4
5. N47S/M121L[a]	355 ± 51	503 ± 5	44.0 ± 2.1	−48 ± 1
6. F114N/M121L[a]	287 ± 34	513 ± 4	~39	~ −66
7. M44F/N47S/F114N/G116F[b]	220 ± 13	588 ± 20	26.8 ± 2.3	−110 ± 7
8. N47S/F114S/M121L[b]	44 ± 5	604 ± 14	30.4 ± 4.3	−110 ± 12
9. N47S/F114N/M121L[a]	78 ± 12	614 ± 11	41.7 ± 5.9	−71 ± 8

[a]Data from ref 43. [b]This study.

dx.doi.org/10.1021/jz5022685 | J. Phys. Chem. Lett. 2015, 6, 100−105

pathways are operating in them and in the WT. Neither pathway involves the mutated residues.

The semiclassical Marcus theory for ET reactions between spatially fixed and oriented donors and acceptors provides a framework for analysis of rate constants in the nonadiabatic regime, eq 1[20]

$$k_{ET} = \kappa(r)\nu \exp(-\Delta G^*/RT) \quad (1)$$

where

$$\Delta G^* = \frac{\lambda_{TOT}}{4}\left[1 + \frac{\Delta G^\circ}{\lambda_{TOT}}\right]^2 \quad (2)$$

In eq 1, $\kappa(r)$ is the transmission coefficient at a separation distance, r, while ν is the frequency of nuclear motions. (In the nonadiabatic regime, $\kappa(r)\nu$ is independent of this frequency.) R and T are the gas constant and temperature (in Kelvins), respectively. ΔG^* and ΔG^0 (cf. eq 2) are the activation free energy and standard free energy of reaction, respectively, and λ_{TOT} is the total reorganization free energies of both the ET donor and acceptor. When the driving force of the reaction equals the total reorganization energy, the rate constant reaches a maximum value, k_{MAX}. Because $\kappa(r)\nu$ decays exponentially with the separation distance, we can calculate k_{MAX} by eq 3

$$k_{max} = \frac{k_B T}{h} \exp[-\beta(r - r_0)] \quad (3)$$

where k_B and h, respectively, are Boltzmann and Planck constants, r is the donor−acceptor separation distance, and r_0 is the value of r for direct (van der Waals) contact; the generally accepted value for r_0 is 0.3 nm. The timetable for activationless electron tunneling in β-sheet proteins of Gray et al. provides a decay constant of β = 10 nm^{-1}.[1]

Attempts to experimentally determine the reduction potential for the formation of the RSS$^{\cdot}$R^{-} radical in azurin have failed so far. Because the cystine is partly solvent-exposed, we have been using a value of −0.41 V versus NHE, determined from hybrid disulfide between a nitroaromatic and a protein cysteine thiol.[44] It is noteworthy that any change in the value for the reduction potential of the disulfide primarily adds or subtracts a constant from the abscissa values of the plot in Figure 2 and thus the reorganization energy by the same value.

The activation free energies, ΔG^*, of the ET reactions in each mutant can be calculated from the activation parameters presented in Table 1. However, the experimentally determined activation entropy, $\Delta S^{\ddagger}$, includes a contribution from the electronic coupling[20]

$$\Delta S^{\ddagger} = \Delta S^* + R \ln(\kappa\nu/10^{13}) = \Delta S^* - R\beta(r - r_0) \quad (4)$$

where the symbols have already been defined.

Figure 3 shows a plot of the ET rate constants, k_{ET}, versus driving force for the nine Az mutants fitted to the theoretical curve calculated using eqs 1 and 2. A nonlinear least-squares analysis of the data yields a value of k_{MAX} = 249(+56/−44) s^{-1} and a reorganization free energy of λ_{TOT} = 0.78(+0.04/−0.04) eV. The broken lines result from using the method of support planes,[45] the limit of each parameter that produces a 10% change in chi squared while the other parameter is allowed to optimize. The two broken lines represent the limits of k_{MAX}. In this analysis, k_{MAX} is the pre-exponential term in eq 1, treated as a constant, and is consistent with a k_{MAX} = 286 s^{-1} calculated directly from eq 3. Also, the reorganization free energies of the individual mutants were calculated independently using the experimental activation parameters, $\Delta H^{\ddagger}$ and $\Delta S^{\ddagger}$. Using $\beta(r - r_0)$ = 23.8 (cf. eq 3), we obtain $R\beta(r - r_0)$ = 198 JK^{-1} mol^{-1} (or 2.05 meV K^{-1}). We then calculate ΔG^* using the activation enthalpy and the corrected activation entropy values. Finally, the reorganization free energy, λ_{calc}, is calculated from eq 2. The results are presented in Table 2.

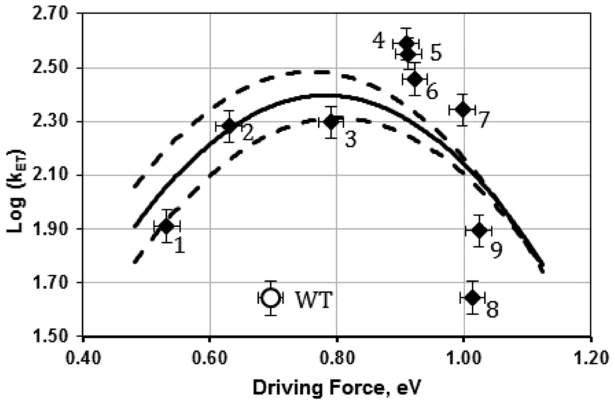

Figure 3. Marcus plot of log(k_{ET}) of intramolecular ET in the Az mutants as a function of the driving force. The fitted line is calculated using k_{MAX} = 249 (+56/−44) s^{-1} and λ_{TOT} = 0.78 (+0.04/−0.04) eV. The points are labeled 1−9, as in Tables 1 and 2. WT Az is the open circle symbol.

As illustrated in Figure 3, the experimentally determined rate constant values of the intramolecular ET in the Az mutants fit the theoretical parabola calculated using Marcus theory in the above plot of the ET rate constants versus their driving force reasonably well, considering the redox potential range of mutants studied and the requirement of k_{MAX} and λ_{TOT} being constant for the entire set of examined mutants. The reorganization energy includes contributions from both the T1 copper site and the disulfide-radical ion. From previous pulse radiolysis studies, we have calculated a λ_{SS} = 1.2 eV,[46,47] which yields a λ_{Cu} = 0.4 eV, a significantly lower value than that (λ_{Cu} = 0.82 eV) previously determined for WT *Pseudomonas aeruginosa* Az.[37] In a previous study, we have attributed such lowering of the reorganization energy to increased flexibility of the T1 copper center caused by changes in noncovalent interactions such as hydrogen bonding and hydrophobicity in the secondary coordination sphere of the T1 copper site.[43] It has been shown before that changing hydrogen bonds and collective perturbation of the protein dynamics can affect the λ values.[48] The deviations from the fit line at the highest driving force would, if attributed only to variation in the reorganization energy, correspond to a variation of up to 0.25 eV from the average or fit value.

The exponential decay constant, β (cf. eqs 3 and 4), is another important parameter determining the ET rates. Differences in β would affect both the ET rates and activation entropies even when a common ET pathway is operating. These differences may be due to subtle changes in the electronic coupling between the copper ion and its ligands, particularly upon slight differences in the covalency of the Cu^{2+}−S(Cys) bond. Calculations of the Fermi contact term presented in Table S1 in the Supporting Information show only small differences in the anisotropic covalency, suggesting that the mutations have only a minor effect on the total electronic coupling along the ET pathway. Furthermore, the electronic coupling between electron donor and acceptor does not change

dx.doi.org/10.1021/jz5022685 | J. Phys. Chem. Lett. 2015, 6, 100−105

Table 2. Reorganization Free Energies, $\lambda_{calc.}$ for the Az Mutants

azurin mutant	$-\Delta G^0$ (eV)	ΔG^* (eV)	$\lambda_{calc.}$ (eV)
1. F114P/M121Q[a]	0.532 ± 0.006	0.033 ± 0.007	0.87
2. F114P[a]	0.630 ± 0.023	∼0.016	0.87
3. F114N*[a]	0.791 ± 0.008	0.009 ± 0.001	0.98
4. N47S/F114N[a]	0.909 ± 0.003	−0.009 ± 0.001	0.91
5. N47S/M121L[a]	0.913 ± 0.005	−0.007 ± 0.006	0.91
6. F114N/M121L[a]	0.923 ± 0.004	∼ −0.003	0.92
7. M44F/N47S/F114N/G116F[b]	0.998 ± 0.020	0.006 ± 0.001	0.85
8. N47S/F114S/M121L[b]	1.014 ± 0.014	0.043 ± 0.005	0.67
9. N47S/F114N/M121L[a]	1.024 ± 0.011	0.040 ± 0.006	0.69

[a]Data from ref 43. [b]This study.

significantly as a result of the mutations (an average $\beta = 10.0 \pm 0.2$ nm^{-1}) and is unlikely to cause the observed steep decrease in rate constants in mutants with the highest driving force illustrated in Figure 3. Comparing mutants 7 and 8, the five-fold decrease in rate constant would require an unlikely change in the decay constant, β, from 10.0 to 10.7. However, minor changes in the electronic coupling could be responsible for the scatter of the points in Figure 3 (beside experimental errors). Examination of the distances in the ET pathways of the different mutants using their crystal structure or molecular dynamics (MD) simulations showed minor differences that do not correlate with the observed rate constants (Table S2 in the Supporting Information).

Taken together, the present results provide rare[49] and compelling evidence that, in this set of Az mutants, the Marcus inverted region has been reached at driving forces greater than ∼0.8 eV (Figure 3). However, the ET rates observed for mutants with the highest driving force lie considerably below the calculated curve. Marcus theory in its semiclassical form attributes the inverted region to an increasing activation energy in the exponential term of the rate equation, but nuclear tunneling may cause a decrease in the pre-exponential factor, leading to the considerably lower rates observed.[50]

These mutants reach the "inverted region" in the internal ET process because they possess a lower reorganization energy than most other Az mutants. When the reorganization energy is higher, as in the case of WT Az (cf. Figure 3), even greater driving force would be required to reach the "inverted region", a rather difficult task to fulfill with modifications of the copper environment. Moreover, the inverted region could be achieved in this system because both ET products, Cu(I) and disulfide, have closed shells and their electronic excited states are too high to be populated after the long-range ET. The inverted region in a bimolecular ET reaction with closed-shell products has indeed been demonstrated before.[51] The present results provide the first demonstration of the Marcus inverted region in a nonderivatized protein-only system. It has been hypothesized that the dramatically different ET rates in the photosynthetic reaction center are due to the lower reorganization free energy and large activation barrier for the reverse processes that result from the inverted region.[27] The inverted region, therefore, allows for the charge separation required for unidirectional ET through that system and is critical for efficient energy conversion processes.

■ ASSOCIATED CONTENT

Supporting Information

Details of experimental procedures, including protein expression and purification, kinetic measurements, cyclic voltammetry analyses, and spectroscopic studies. This material is available free of charge via the Internet at http://pubs.acs.org.

■ AUTHOR INFORMATION

Corresponding Author

*E-mail: yi-lu@illinois.edu.

Notes

The authors declare no competing financial interest.

■ ACKNOWLEDGMENTS

This work is supported by the U.S. National Science Foundation (CHE-1413328 to Y.L.). O.F. acknowledges the generous support extended by the Kimmelman Center for Biomolecular Structure and Assembly at the Weizmann Institute of Science. We also thank Ms. Nilly Hafezi for technical help.

■ REFERENCES

(1) Gray, H. B.; Winkler, J. R. Electron Transfer in Proteins. *Annu. Rev. Biochem.* **1996**, *65*, 537−561.

(2) Farrar, J. A.; Neese, F.; Lappalainen, P.; Kroneck, P. M. H.; Saraste, M.; Zumft, W. G.; Thomson, A. J. The Electronic Structure of Cu_A: A Novel Mixed-Valence Dinuclear Copper Electron-Transfer Center. *J. Am. Chem. Soc.* **1996**, *118*, 11501−115114.

(3) Farver, O.; Kroneck, P. M. H.; Zumft, W. G.; Pecht, I. Intramolecular Electron Transfer in Cytochrome cd_1 Nitrite Reductase from Pseudomonas stutzeri; Kinetics and Thermodynamics. *Biophys. Chem.* **2002**, *98*, 27−34.

(4) Farver, O.; Kroneck, P. M. H.; Zumft, W. G.; Pecht, I. Allosteric Control of Internal Electron Transfer in Cytochrome cd_1 Nitrite Reductase. *Proc. Natl. Acad. Sci. U. S. A.* **2003**, *100*, 7622−7625.

(5) Hudson, J. M.; Heffron, K.; Kotlyar, V.; Sher, Y.; Maklashina, E.; Cecchini, G.; Armstrong, F. A. Electron Transfer and Catalytic Control by the Iron-Sulfur Clusters in a Respiratory Enzyme, E. coli Fumarate Reductase. *J. Am. Chem. Soc.* **2005**, *127*, 6977−6989.

(6) Farver, O.; Pecht, I. Elucidation of Electron-Transfer Pathways in Copper and Iron Proteins by Pulse Radiolysis Experiments *Prog. Inorg. Chem.* **2007**, *55*, 1−78.

(7) Davidson, V. L. Protein Control of True, Gated, and Coupled Electron Transfer Reactions. *Acc. Chem. Res.* **2008**, *41*, 730−738.

(8) Liu, J.; Chakraborty, S.; Hosseinzadeh, P.; Yu, Y.; Tian, S.; Petrik, I.; Bhagi, A.; Lu, Y. Metalloproteins Containing Cytochrome, Iron-Sulfur, or Copper Redox Centers. *Chem. Rev.* **2014**, *114*, 4366−4469.

(9) Winkler, J. R.; Gray, H. B. Electron Flow through Metalloproteins. *Chem. Rev.* **2014**, *114*, 3369−3380.

(10) Moser, C. C.; Farid, T. A.; Chobot, S. E.; Dutton, P. L. Electron Tunneling Chains of Mitochondria. *Biochim. Biophys. Acta, Bioenerg.* **2006**, *1757*, 1096−1109.

(11) Moser, C. C.; Anderson, J. L. R.; Dutton, P. L. Guidelines for Tunneling in Enzymes. *Biochim. Biophys. Acta, Bioenerg.* **2010**, *1797*, 1573−1586.

(12) Abriata, L. A.; Alvarez-Paggi, D.; Ledesma, G. N.; Blackburn, N. J.; Vila, A. J.; Murgida, D. H. Alternative Ground States Enable Pathway Switching in Biological Electron Transfer. *Proc. Natl. Acad. Sci. U. S. A.* **2012**, *109*, 17348−17353.
(13) DeBeer George, S.; Basumallick, L.; Szilagyi, R. K.; Randall, D. W.; Hill, M. G.; Nersissian, A. M.; Valentine, J. S.; Hedman, B.; Hodgson, K. O.; Solomon, E. I. Spectroscopic Investigation of Stellacyanin Mutants: Axial Ligand Interactions at the Blue Copper Site. *J. Am. Chem. Soc.* **2003**, *125*, 11314−11328.
(14) van der Felt, C.; Hindoyan, K.; Choi, K.; Javdan, N.; Goldman, P.; Bustos, R.; Star, A. G.; Hunter, B. M.; Hill, M. G.; Nersissian, A.; Udit, A. K. Electron-Transfer Rates Govern Product Distribution in Electrochemically-Driven P450-Catalyzed Dioxygen Reduction. *J. Inorg. Biochem.* **2011**, *105*, 1350−1353.
(15) Bandi, S.; Bowler, B. E. A Cytochrome *c* Electron Transfer Switch Modulated by Heme Ligation and Isomerization of a Peptidyl-Prolyl Bond. *Biopolymers* **2013**, *100*, 114−124.
(16) McMillan, D. G. G.; Marritt, S. J.; Firer-Sherwood, M. A.; Shi, L.; Richardson, D. J.; Evans, S. D.; Elliott, S. J.; Butt, J. N.; Jeuken, L. J. C. Protein-Protein Interaction Regulates the Direction of Catalysis and Electron Transfer in a Redox Enzyme Complex. *J. Am. Chem. Soc.* **2013**, *135*, 10550−10556.
(17) Zhong, F.; Lisi, G. P.; Collins, D. P.; Dawson, J. H.; Pletneva, E. V. Redox-Dependent Stability, Protonation, and Reactivity of Cysteine-Bound Heme Proteins. *Proc. Natl. Acad. Sci. U. S. A.* **2014**, *111*, E306−E315.
(18) Gu, J.; Yang, S.; Rajic, A. J.; Kurnikov, I. V.; Prytkova, T. R.; Pletneva, E. V. Control of Cytochrome *c* Redox Reactivity through Off-Pathway Modifications in the Protein Hydrogen-Bonding Network. *Chem. Commun.* **2014**, *50*, 5355−5357.
(19) Bak, D. W.; Elliott, S. J. Alternative FeS Cluster Ligands: Tuning Redox Potentials and Chemistry. *Curr. Opin. Chem. Biol.* **2014**, *19*, 50−58.
(20) Marcus, R. A.; Sutin, N. Electron Transfers in Chemistry and Biology. *Biochim. Biophys. Acta, Rev. Bioenerg.* **1985**, *811*, 265−322.
(21) Beratan, D. N.; Onuchic, J. N.; Winkler, J. R.; Gray, H. B. Electron-Tunneling Pathways in Proteins. *Science* **1992**, *258*, 1740−1741.
(22) Miller, J. R.; Calcaterra, L. T.; Closs, G. L. Intramolecular Long-Distance Electron Transfer in Radical Anions. The Effects of Free Energy and Solvent on the Reaction Rates. *J. Am. Chem. Soc.* **1984**, *106*, 3047−3049.
(23) Fox, L. S.; Kozik, M.; Winkler, J. R.; Gray, H. B. Gaussian Free-Energy Dependence of Electron-Transfer Rates in Iridium Complexes. *Science* **1990**, *247*, 1069−1071.
(24) Scott, J. R.; Willie, A.; McLean, M.; Stayton, P. S.; Sligar, S. G.; Durham, B.; Millett, F. Intramolecular Electron Transfer in Cytochrome b_5 Labeled with Ruthenium(II) Polypyridine Complexes: Rate Measurements in the Marcus Inverted Region. *J. Am. Chem. Soc.* **1993**, *115*, 6820−6824.
(25) Winkler, J. R.; Malmstroem, B. G.; Gray, H. B. Rapid Electron Injection into Multisite Metalloproteins: Intramolecular Electron Transfer in Cytochrome Oxidase. *Biophys. Chem.* **1995**, *54*, 199−209.
(26) Gunner, M. R.; Dutton, P. L. Temperature and -ΔG° Dependence of the Electron Transfer from BPh·- to QA in Reaction Center Protein from Rhodobacter sphaeroides with Different Quinones as QA. *J. Am. Chem. Soc.* **1989**, *111*, 3400−3412.
(27) Marcus, R. A. Electron-Transfer Reactions in Chemistry: Theory and Experiment (Nobel lecture). *Angew. Chem.* **1993**, *105*, 1161−1172.
(28) Farver, O.; Skov, L. K.; Gilardi, G.; van Pouderoyen, G.; Canters, G. W.; Wherland, S.; Pecht, I. Structure-Function Correlation of Intramolecular Electron Transfer in Wild Type and Single-Site Mutated Azurins. *Chem. Phys.* **1996**, *204*, 271−277.
(29) Kuznetsov, A. M.; Ulstrup, J. A Theory of Electron Transfer in Bridged and Supramolecular Systems. *J. Inclusion Phenom. Macrocyclic Chem.* **1999**, *35*, 45−54.
(30) Gray, H. B.; Malmstrom, B. G.; Williams, R. J. P. Copper Coordination in Blue Proteins *JBIC. J. Biol. Inorg. Chem.* **2000**, *5*, 551−559.
(31) Ryde, U.; Olsson, M. H. M.; Pierloot, K. The Structure and Function of Blue Copper Proteins. *Theor. Comput. Chem.* **2001**, *9*, 1−55.
(32) Kolczak, U.; Dennison, C.; Messerschmidt, A.; Canters, G. W. In *Handbook of Metalloproteins*; Messerschmidt, A., Ed.; John Wiley & Sons Ltd.: Chichester, U.K., 2001; Vol. *2*, pp 1170−1194.
(33) Vila, A. J.; Fernandez, C. O. Copper in Electron Transfer Proteins, In *Handbook of Metalloproteins*; Messerschmidt, A., Bertini, I., Sigel, A., Sigel, H., Eds.; Wiley: New York, 2001; Vol. *1*, pp 813−856.
(34) Solomon, E. I.; Szilagyi, R. K.; DeBeer George, S.; Basumallick, L. Electronic Structures of Metal Sites in Proteins and Models: Contributions to Function in Blue Copper Proteins. *Chem. Rev.* **2004**, *104*, 419−458.
(35) Lu, Y. Electron Transfer: Cupredoxins, In *Comprehensive Coordination Chemistry II*; Elsevier, Ltd.: Boston, 2004; Vol. *8*, pp 91−122.
(36) Pascher, T.; Karlsson, B. G.; Nordling, M.; Malmstroem, B. G.; Vaenngaard, T. Reduction Potentials and their pH Dependence in Site-Directed-Mutant forms of Azurin from Pseudomonas aeruginosa. *Eur. J. Biochem.* **1993**, *212*, 289−296.
(37) Di Bilio, A. J.; Hill, M. G.; Bonander, N.; Karlsson, B. G.; Villahermosa, R. M.; Malmstroem, B. G.; Winkler, J. R.; Gray, H. B. Reorganization Energy of Blue Copper: Effects of Temperature and Driving Force on the Rates of Electron Transfer in Ruthenium- and Osmium-Modified Azurins. *J. Am. Chem. Soc.* **1997**, *119*, 9921−9922.
(38) Berry, S. M.; Ralle, M.; Low, D. W.; Blackburn, N. J.; Lu, Y. Probing the Role of Axial Methionine in the Blue Copper Center of Azurin with Unnatural Amino Acids. *J. Am. Chem. Soc.* **2003**, *125*, 8760−8768.
(39) Yanagisawa, S.; Banfield, M. J.; Dennison, C. The Role of Hydrogen Bonding at the Active Site of a Cupredoxin: The Phe114Pro Azurin Variant. *Biochemistry* **2006**, *45*, 8812−8822.
(40) Garner, D. K.; Vaughan, M. D.; Hwang, H. J.; Savelieff, M. G.; Berry, S. M.; Honek, J. F.; Lu, Y. Reduction Potential Tuning of the Blue Copper Center in Pseudomonas aeruginosa Azurin by the Axial Methionine as Probed by Unnatural Amino Acids. *J. Am. Chem. Soc.* **2006**, *128*, 15608−15617.
(41) Lancaster, K. M.; Farver, O.; Wherland, S.; Crane, E. J., III; Richards, J. H.; Pecht, I.; Gray, H. B. Electron Transfer Reactivity of Type Zero Pseudomonas aeruginosa Azurin. *J. Am. Chem. Soc.* **2011**, *133*, 4865−4873.
(42) Marshall, N. M.; Garner, D. K.; Wilson, T. D.; Gao, Y.-G.; Robinson, H.; Nilges, M. J.; Lu, Y. Rationally Tuning the Reduction Potential of a Single Cupredoxin Beyond the Natural Range. *Nature* **2009**, *462*, 113−116.
(43) Farver, O.; Marshall, N. M.; Wherland, S.; Lu, Y.; Pecht, I. Designed Azurins Show Lower Reorganization Free Energies for Intraprotein Electron Transfer. *Proc. Natl. Acad. Sci. U. S. A.* **2013**, *110*, 10536−10540.
(44) Faraggi, M.; Klapper, M. H. Intramolecular Long-Range Electron Transfer in the α-Hemoglobin Subunit. *J. Am. Chem. Soc.* **1988**, *110*, 5753−5756.
(45) Duggleby, R. G. Estimation of the Reliability of Parameters Obtained by Non-Linear Regression. *Eur. J. Biochem.* **1980**, *109*, 93−96.
(46) Farver, O.; Lu, Y.; Ang, M. C.; Pecht, I. Enhanced Rate of Intramolecular Electron Transfer in An Engineered Purple Cu_A Azurin. *Proc. Natl. Acad. Sci. U. S. A.* **1999**, *96*, 899−902.
(47) Farver, O.; Pecht, I. Electron Transfer in Blue Copper Proteins. *Coord. Chem. Rev.* **2011**, *255*, 757−773.
(48) Alvarez-Paggi, D.; Castro, M. A.; Tórtora, V.; Castro, L.; Radi, R.; Murgida, D. H. Electrostatically Driven Second-Sphere Ligand Switch between High and Low Reorganization Energy Forms of Native Cytochrome c. *J. Am. Chem. Soc.* **2013**, *135*, 4389−4397.
(49) Boussac, A.; Rappaport, F.; Brettel, K.; Sugiura, M. Charge Recombination in SnTyrZ$^{\bullet}$QA$^{-\bullet}$ Radical Pairs in D1 Protein Variants

of Photosystem II: Long Range Electron Transfer in the Marcus Inverted Region. *J. Phys. Chem. B* **2013**, *117*, 3308−3314.
(50) Liang, N.; Miller, J. R.; Closs, G. L. Temperature-Independent Long-Range Electron Transfer Reactions in the Marcus Inverted Region. *J. Am. Chem. Soc.* **1990**, *112*, 5353−5354.
(51) McCleskey, T. M.; Winkler, J. R.; Gray, H. B. Driving-Force Effects on the Rates of Bimolecular Electron-Transfer Reactions. *J. Am. Chem. Soc.* **1992**, *114*, 6935−6937.